SCIENCE CHINA
Information Sciences

• RESEARCH PAPERS •

November 2011 Vol. 54 No. 11: 2324–2337
doi: 10.1007/s11432-011-4308-6

Statistical approach to weak signal detection and estimation using Duffing chaotic oscillators

JIN Tian* & ZHANG Hua

School of Electronic Information Engineering, BeiHang University, Beijing 100191*, China*

Received April 12, 2010; accepted October 19, 2010; published online August 7, 2011

Abstract In this paper, we describe the statistical characteristics of weak signal detection by a chaotic Duffing oscillator, and present a new method for signal detection and estimation using the largest Lyapunov exponent. Previous research has shown that weak signals can be detected by a chaotic system. Many researchers use the Lyapunov exponent to flag the detection of a chaotic state, but our research shows that the Lyapunov exponent follows statistical characteristics, and therefore more factors should be considered in flagging chaotic weak signals. Here, we analyze the statistical characteristics inherent in the Lyapunov exponent calculation steps, and build up a statistical model for different chaotic states based on simulation data. Furthermore, we provide expressions for false-alarm and detection probabilities, selection of driving force threshold and detection of signal-noise-ratio. Finally, we summarize the method of signal amplitude estimation. Our research indicates that the performance of the detection system is related to sampling times and intervals, in accord with the theory of statistical signal detection.

Keywords weak signal detection, Lyapunov exponent, chaos, Duffing oscillation, statistical signal process

Citation Jin T, Zhang H. Statistical approach to weak signal detection and estimation using Duffing chaotic oscillators. Sci China Inf Sci, 2011, 54: 2324–2337, doi: 10.1007/s11432-011-4308-6

1 Introduction

Recently, weak signal detection using chaotic oscillators has been widely studied in the field of signal processing. In 1992, Birx made pioneering experiments on signal detection in noisy environments [1]. In 1995, Haykin used artificial neural network methods to extract weak signals from chaotic noise background [2]. In 1996, Leung used minimum phase space volume (MPSV) methods to estimate the autoregressive (AR) model inside chaotic noise [3]. As early as 1997, Short and Kennedy showed how to extract signals from chaotic communications [4, 5]. In 1999, Wang used a chaotic oscillator to detect sinusoidal signals from white noise with −66 dB SNR [6]. Later, he investigated the method of estimating signal phase and amplitude based on a chaotic oscillator [7]. In 2001, Wang extracted the original signal from background noise by this method [8]. From 2003 to 2008, Li performed a series of experiments [9–11] on frequency and amplitude signal detection, lowering the SNR to −111 dB. In 2009, Liu analyzed the detection method of weak periodic signals by using a chaotic oscillator [12]. Our research shows that the previous paper had not considered that the chaotic decision flag could be subjected to noise interference, and also had

*Corresponding author (email: jintian@buaa.edu.cn)

not studied the probability of missing and false detections. The conclusion is that the SNR cannot be used to measure the system performance.

Because the chaotic oscillator is impervious to white noise but sensitive to signals, any weak signal will pull the system out from its chaotic state. If this weak signal affects the phase portrait, it can be detected. There are two ways to check that a system is in a chaotic state or not: one is by visual analysis and the other analytic. Visual analysis is rather subjective and is difficult to extend to an engineering arena. Analytical methods use special characteristic values to judge whether states are chaotic. These characteristic values identifying chaotic behavior include fractal dimensions [13], Kolmogorov entropy [14] and Lyapunov exponents [15]; the first two are hard to calculate, but are related to the Lyapunov exponent. Most researchers focus on the largest Lyapunov exponent as a quantitative check in weak signal detection [16–18]. Although signal detection is a stochastic problem, no one has analyzed the stochastic behavior of Lyapunov exponents. Despite the fact that the Lyapunov exponent has been found to have a failure probability [16, 19], no further research in this area has been pursued.

Our study uses statistical theory of signal detection to analyze the statistical characteristics of the Lyapunov exponent in weak signal detection. We first develop the statistical model of these exponents, and reveal their relationship to false alarms and detection probabilities. Our research shows for the first time that chaos signal detection and statistical detection can exploit similar models, and proves that the Lyapunov exponent is not a deterministic flag of weak signal detection. Additionally, our study also extends the method to signal amplitude estimation. The statistical signal model could be also used in chaotic estimations, bringing a novel way to treat weak signal estimations by means of a chaotic oscillator.

2 Weak signal detection based on the Duffing chaotic oscillator

2.1 Duffing oscillator and phase portrait

The Duffing oscillator was introduced into nonlinear dynamics by Duffing in 1918. However, the modified Duffing-Holmes equation is the preferred and widely used form in weak signal detection [16, 20]. This is expressed as follows

$$x'' + kx' - ax^3 + bx^5 = F\cos(\omega t), \tag{1}$$

The dynamic equation is shown in (2):

$$\begin{cases} x' = y, \\ y' = -ky + ax^3 - bx^5 + F\cos(\omega t), \end{cases} \tag{2}$$

where k is damping factor, a and b are two real numbers, and F is periodic driving force. The physical meaning of (2) is that it describes a non-linear vibrational equation with polynomial resilience. With different F, the system falls into one of five different states, classified as either homoclinic, bifurcation, chaotic, critical, or large-scale periodic. Weak signal detection uses the chaotic, critical and large-scale period states, phase portraits of which are shown in Figure 1.

According to Wang [21], changes in the chaotic state are immune to noise. This is mainly because of the following three reasons. The first is that the non-linear gain of the system enables weak signals to be different from background noise. The second is the presence of noise suppression in the periodic state. The third is related to the sampling integrator. According to the statistical characteristic of the right-most point R in the phase portrait, Wang concluded that the SNR of point R can be defined by

$$\mathrm{SNR}_0 = \frac{\sqrt{m}x_a}{\sigma} = \frac{\sqrt{m}x_a}{\sqrt{0.48h}\sigma_0}, \tag{3}$$

and the input SNR of amplitude by

$$\mathrm{SNR}_1 = \frac{A}{\sigma_0}. \tag{4}$$

Therefore, the SNR of the energy improvement by the non-linear gain is

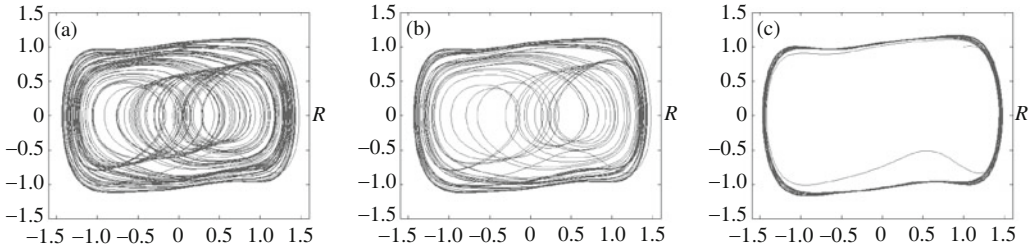

Figure 1 Phase portraits of the chaotic system. (a) Chaotic states; (b) critical states; (c) large-scale periodic states.

$$\mathrm{SNIR} = 20\log\left(\frac{x_a}{A}\sqrt{\frac{m}{0.48h}}\right), \tag{5}$$

where A is the amplitude of input signal, x_a the x-coordination of the right-most point R, m the sampling integrator count, h the sample interval, σ_0 the standard deviation of input noise, and σ the standard deviation of point R. According to Wang's result, when the amplitude of the input signal is 0.01, the sample interval is 0.001, with x_a equal to 1.71. Even when there is one sampling integrator, the SNR improvement could be 77.8 dB. However, the detection of weak signals is based on a state change, not on a point value in a phase portrait. Thus, the improvement of the SNR is important for noise suppression, but is not significant for signal detection.

2.2 Lyapunov exponent

As previously mentioned, the visual analysis of a phase portrait state change is not feasible in an engineering context. The basic characteristic of chaotic motion is its sensitivity to initial conditions. Two orbits generated from two close initial values will part from each other exponentially. The Lyapunov exponent provides a quantitative description of this behavior [15]. Consider two (usually nearest) neighboring points in phase space at initial time 0 and at later time t, with the distances of the points in the i-th direction being $\|\delta x_i(0)\|$ and $\|\delta x_i(t)\|$, respectively. The Lyapunov exponent is then defined as the average growth rate λ_i of the initial distance

$$\frac{\|\delta x_i(t)\|}{\|\delta x_i(0)\|} = e^{\lambda_i t}(t \to \infty), \tag{6}$$

or equivalently

$$\lambda_i = \lim_{t\to\infty}\frac{1}{t}\ln\frac{\|\delta x_i(t)\|}{\|\delta x_i(0)\|}. \tag{7}$$

For the chaos detection phase portrait depicted in Figure 1, there are two Lyapunov exponents, the sum of the two exponents being $-k$. The chaotic state of the system can be tested by the largest Lyapunov exponent [22]. If the largest Lyapunov exponent is positive, all differences in the orbit will change chaotically whatever the initial distances are. In contradistinction, if the largest Lyapunov exponent is negative, differences in the orbit will disappeared. The system's state will remain in a large-scale periodic orbit, indicating that there exists a weak signal. Because the Lyapunov exponent has good quantitative characteristics, it is also useful in the selection of driving force threshold F_r.

Calculations of Lyapunov exponents in continuous systems are mainly performed by one of several means including the definition method, Jacobian matrix method, Wolf method [23], and small data set method [24]. If the system's dynamic equation is known, the definition method and Jacobian matrix method are commonly used; otherwise, the Wolf method and small data set method are used. In our case this equation is known, and hence to calculate Lyapunov exponents we have elected to use the Jacobian matrix method. The detailed steps are as follows:

For a continuous system, $x' = D(x)$, where $x' = \frac{\mathrm{d}x}{\mathrm{d}t}$. The x value in the phase portrait is frustrated by input noise n_σ. The continuous tangent space has a point $x(t)$ at which a tangent vector e can be described by following formula:

$$e' = J(x(t))e, \tag{8}$$

where $J = \frac{\partial D}{\partial x}$. Here, J is the Jacobian matrix of function $D(x)$. Let $e(0) \to e(t)$ be a continuous linear operator in the mapping variable U. The function can be written as

$$e(t) = U(t, e(0)). \tag{9}$$

The evolution of U can be described by the exponent from Jacobian matrix, that is,

$$\lambda(x(0), e(0)) = \lim_{t\to\infty} \frac{1}{t} \ln \frac{\|e(t)\|}{\|e(0)\|}. \tag{10}$$

The average value of the evolution can be represented by

$$\lambda = \lim_{t\to\infty} \frac{1}{k\Delta t} \sum_{j=1}^{k} \ln \frac{\|e((j+1)\Delta t)\|}{\|e(j\Delta t)\|}. \tag{11}$$

(11) is fundamental to the Jacobian matrix method in calculating the Lyapunov exponent in a continuous system. Here, we have defined the sample interval $h = \Delta t$, and sampling time $n = k\Delta t$.

2.3 Traditional weak signal detection by chaotic oscillator

In his paper, Wang gave originally the three main steps involved in weak signal detection using a chaotic oscillator [6]. The first step is to fix the dumping factor k in (1), and increase the driving force F step by step, until the chaotic phase portrait state changes into a critical state. The critical state is an intermediate state between a chaotic state and a large-scale periodic state; if F is increased further, the state will exhibit large-scale periodicity. Typical phase portraits of these three states are shown in Figure 1. Testing of a critical state is determined by its Lyapunov exponent. The second step is to mark the driving force threshold $F_r = F$, and record the Duffing equation with the threshold value. The third step involves generating the input signal $S(t)$ with a periodical signal frequency equal or close to the driving force frequency ω. The signal will be detected even if the background noise is very high. The new equations are shown in (12):

$$\begin{aligned} &x'' + kx' - ax^3 + bx^5 = F_r \cos(\omega t) + S(t), \\ &S(t) = A\cos(\omega t) + n_\sigma(t), \end{aligned} \tag{12}$$

where A is the amplitude of the periodic input signal, $n_\sigma \sim N(0, \sigma_0^2)$, and σ_0 the standard deviation of the noise signal. If there exists a periodic input signal, even if $A \ll \sigma_0$, the phase portrait will change from one characterizing chaotic behavior to one for large-scale periodic motion. According to Li et al. [11], the detection SNR of a sinusoidal input signal can be -110 dB, which means

$$10 \log \frac{A^2}{\sigma_0^2} = -110 \text{ dB}.$$

3 Statistical characteristics of the Lyapunov exponent

The key problem in previous research is that the noise interference on the chaotic test was not taken into consideration. The direct use of the Lyapunov exponent as a criterion will lead to a higher missing probability. In this section, we will analyze the factors affecting the calculation of the Lyapunov exponent by theoretical methods, and focus on the relationship between the driving force and the Lyapunov exponent under the three different states. Finally, a model developed to investigate the relations between input noise and Lyapunov exponent will be established in a simulation.

3.1 Non-linear gain of chaotic system

As we discussed above, the non-linear gain of a chaotic system cannot be used as a criterion in weak signal detection. Instead, the Lyapunov exponent is commonly used in testing for a change in a chaotic state. Although the Lyapunov exponent is proved to be a good quantitative criterion with high gain, it is still affected by frustration in a phase orbit caused by signal noise. Thus, the calculated Lyapunov exponent will no longer be a definitive test. When considering the right-most point R in a phase portrait, $x' = 0$, $x'' \approx 0$. The input noise σ_0 will be added to F_r after multiplying by the factor $\sqrt{0.48h}$, that will also cause the state to change. Consequently, studying the statistical characteristics of F_r and the Lyapunov exponent will reveal the relationship between the input signal and Lyapunov exponent. From the discussions above, the difference between the standard deviations of coordination x (represented by σ_x) and input noise (represented by σ_0) is the multiplicative factor $\sqrt{0.48h}$. Thus, a reduction in the sampling interval h will be helpful in decreasing the standard deviation of the phase portrait.

3.2 Theoretical analysis of the Lyapunov exponent in statistical characteristics

For critical and large-scale period states, the factors affecting the evaluation of Lyapunov exponents include: sampling interval h, sampling time n, inputted noise σ_0, driving force threshold F_r and input signal A. This interference can be treated as yet another noise caused by the input signal noise.

With regard to sampling interval h, it has been proved that the variance of the phase portrait is directly rated to h [21]. Eq. (12) describes a system with an inputted noisy signal with variation σ_0^2. According to Wang et al. [21], the phase portrait noise σ_x^2 is proportion to the input noise. In this paper, we use r_1 as the ratio of two noises, as expressed in (13):

$$\sigma_x^2 = r_1(t) \times h \times \sigma_0^2. \tag{13}$$

Focusing now on the sampling time n, the standard deviation of Lyapunov exponent will decrease with increasing n. Although the noise distribution of $\lim_{t\to\infty} \frac{1}{t} \ln \frac{\|e(t)\|}{\|e(0)\|}$ cannot be calculated, the Lyapunov exponent is according to (11) the sum of n random variables. Applying the central limit theory, if each variable is only slightly affected and none is critical, the sum of the variables follows a normal distribution [25]. Because each variable $\ln \frac{\|e((j+1)\Delta t)\|}{\|e(j\Delta t)\|}$ only contributes slightly to the sum, the Lyapunov exponent will follow a normal distribution, and the standard deviation will decrease with increasing n. Denoting the variance of Lyapunov exponent by σ_λ^2, we express the variance in the form

$$\sigma_\lambda^2 = \frac{r_2 \times \sigma_x^2}{n}. \tag{14}$$

When the system is in a chaotic state, the dynamics as expressed by (12), is impervious to any input signal. Thus, the input signal does not affect the variance of the phase portrait σ_x^2 which can be considered as a normal distribution value irrespective of the input signal. In this paper, we use r_3 to denote the constant of proportionality between σ_x^2 and n_0^2:

$$\sigma_x^2 = r_3 \times n_0^2. \tag{15}$$

Figure 2 displays phase portraits obtained from simulations with inputted noise. Compared with Figure 1, these phase portraits clearly exhibit more frustration.

According to the above analysis, noise σ_0 can be treated as a small perturbation f to the driving force F, which ultimately modifies the Lyapunov exponent condition. Because f is an equivalent estimation, it cannot be deduced by theory. Instead, the relationship between the driving force and the input noise will be analyzed by statistical means.

When a weak input signal is present, (12) simplifies to (16):

$$\begin{aligned} x'' + kx' - ax^3 + bx^5 &= F_r \cos(\omega t) + A\cos(\omega t) + \sigma_0 \mathrm{rand}n(t) \\ &= (F_r + A)\cos(\omega t) + \sigma_0 \mathrm{rand}n(t). \end{aligned} \tag{16}$$

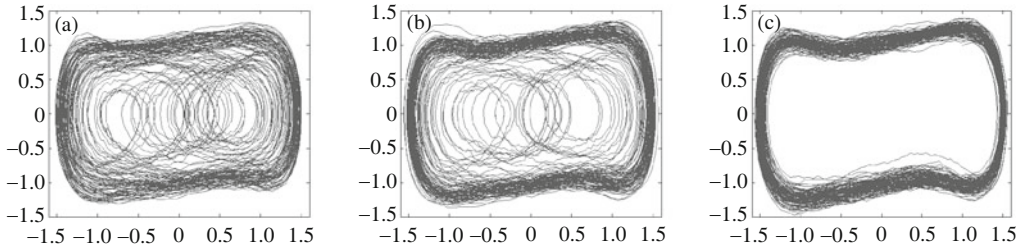

Figure 2 Phase portraits of a chaotic system affected by noise. (a) Chaotic states; (b) critical states; (c) large-scale periodic states.

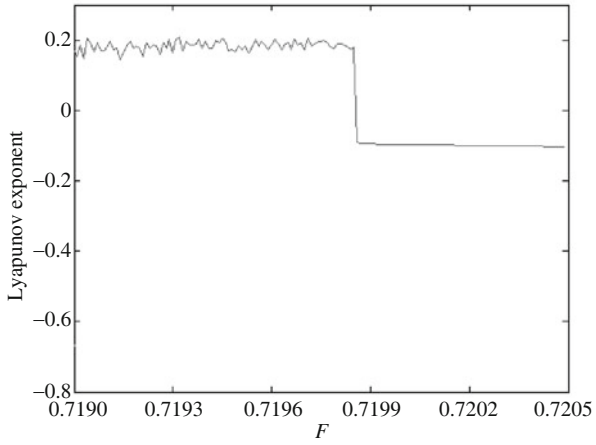

Figure 3 Relationship between largest Lyapunov exponent of a Duffing oscillator and driving force.

Table 1 Value of driving force threshold in different parameters

h	n	F_r
0.01	100	0.719854757750137
0.001		0.71859405144014
0.0001		0.71848972929516
0.01	1000	0.719854757750121
	10000	0.719854757750121

With the effect of a weak signal finally added to the driving force F_r, the chaotic system changes state and the Lyapunov exponent becomes negative.

3.3 Statistical model of the Lyapunov exponent

3.3.1 *Relationship between Lyapunov exponent and driving force*

When there is no input signal, the relationship between the driving force F and largest Lyapunov exponent is shown in Figure 3. The transition position of the Lyapunov exponent is the critical state. The left and right sides correspond to chaotic and large-scale periodic states, respectively.

Simulations show that the value of F_r is related by the vibration equation to parameters n and h. Based on (12), the value of F_r given different parameter values are shown in Table 1.

When h=0.01 and n=100, two values F_1 and F_2 are selected either side of the driving force values, F_1=0.71985475775012 and F_2=0.71985475775014. As Figure 3 shows, when $F < F_1$, the system is in a chaotic state; when $F \geqslant F_2$, the system is in large-scale periodic state; when $F_1 \leqslant F < F_2$, the system

is in critical state. For each of these different states, the contribution of noise to the Lyapunov exponent can be represented by n_c, n_p and n_l, so that we can express the Lyapunov exponent in these states by following three formulas:

$$\begin{cases} \lambda_1 = \lambda_c + n_c & F < F_1, \\ \lambda_2 = \lambda_p + n_p & F_1 \leqslant F < F_2, \\ \lambda_3 = \lambda_l + n_l & F \geqslant F_2. \end{cases} \tag{17}$$

Here, λ_1, λ_2 and λ_3 represent the Lyapunov exponent value for the chaotic, critical and large-scale states, respectively.

3.3.2 *Statistical characteristics of the Lyapunov exponent for a chaotic state*

In the chaotic state, the largest Lyapunov exponent follows a normal distribution for which the mathematical expectation is non-zero. The mean value of λ_c is constant, independent F_r and σ_0. This is because the vibration equation is impervious to the inputted noise that stabilizes the variance of the Lyapunov exponent. Actually, the stability of the variance is because this variance in the chaotic state is much higher than that incurred by the input noise, making the system seemingly impervious to noise. The system transitions from the chaotic state to either a homoclinic state or a large-scale period state as the input noise increases.

When we put (14) and (15) into (17), the relationship between input noise and Lyapunov exponent could be represented by formula:

$$\lambda_1 = \lambda_c + n_c = \lambda_c + \frac{R_c}{\sqrt{n}} n_0, \tag{18}$$

where λ_c is the average value of the Lyapunov exponent in the chaotic state, n_c its frustration, n_0 the Gaussian white noise follows $N(0,1)$, R_c the chaotic ratio to input noise, and n the sampling time. The statistical results are shown in Table 2. When $k = 0.5$ and $\sigma_0^2 = 10^{-6}$, the parameters in (18) are: $\lambda_c = 0.1815$ and $R_c = 0.137$. Because λ_c is 10 times the standard deviation, the Lyapunov exponent will not become negative in this situation.

The Lyapunov exponent distribution for a chaotic state is shown in Figure 4.

3.3.3 *Statistical characteristics of the Lyapunov exponent for a large-scale periodic state*

The largest Lyapunov exponent for a large-scale periodic state follows a normal distribution for which the mathematical expectation is non-zero. The average value is λ_l. In contradistinction to chaotic states, λ_l is not constant and is linear in F_r. The variance is proportional to the sampling time n and inversely proportional to the input noise. This signifies that the Lyapunov exponent for a large-scale periodic state is sensitive to noise.

When we put (13) and (14) into (17), the Lyapunov exponent for such states with perturbing input noise can be represented by (19).

$$\lambda_3 = \lambda_l + n_l = \lambda_l + \frac{R_l\sqrt{h}}{\sqrt{n}} n_\sigma, \tag{19}$$

where λ_l is the average value of the Lyapunov exponent for the large-scale periodic state, n_l its frustration, and R_l its ratio to input noise. Moreover, λ_l is a variable that depends on the driving force threshold F_r. Statistical results show that when k=0.5, h=0.01 and n=100, the parameters in (19) are: $\lambda_l = -0.1005$, and $R_l = 19.1$. Because λ_l is 10 times the standard deviation, the Lyapunov exponent will not become positive in this situation.

The relationship between λ_l and F_r can be acquired by linear fitting. The formula is:

$$\lambda_l = -a_l F_r + b_l, \tag{20}$$

Table 2 Statistic results of the Lyapunov exponent for a chaotic state

F_r	h	n	Mean value	Standard deviation
0.7193	0.01	100	0.1815	0.0140
0.7185	0.001		0.1803	0.0138
0.7180	0.0001		0.1838	0.0135
0.7193	0.01	1000	0.1835	0.0040
		10000	0.1839	0.0013

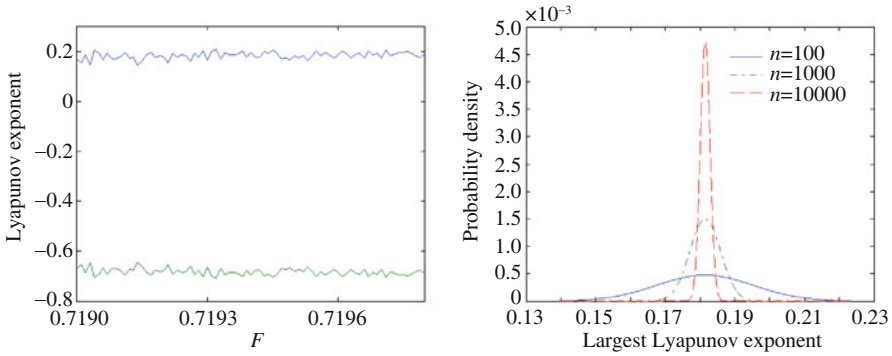

Figure 4 Lyapunov exponent distribution for a chaotic state.

Table 3 Statistic results of the Lyapunov exponent for a large-scale periodic state

F_r	h	n	σ_0	Mean value	Standard deviation
0.7203	0.01	100	10^{-6}	−0.1005	1.91e−4
0.7195	0.001			−0.0989	1.07e−4
0.7190	0.0001			−0.0963	5.22e−5
0.7203	0.01	1000	10^{-6}	−0.1014	5.59e−5
		10000		−0.1015	1.80e−5
0.7203	0.01	100	10^{-7}	−0.1005	6.67e−5
			10^{-8}	−0.1005	2.04e−5

where a_l and b_l are fitting parameters. According to the statistical results for the driving forces from 0.7199 to 0.7205, these parameters were found to be $a_l = 12.2809$ and $b_l = 8.7454$.

Putting (20) into (19) yields the Lyapunov exponent formula for a large-scale periodic state.

$$\lambda_3 = -a_l F + b_l + \frac{R_l\sqrt{h}}{\sqrt{n}}\sigma_0. \tag{21}$$

If the perturbing input noise is of the same order as the frustration to driving force, the relationship between these is:

$$\sigma_F = \frac{R_l\sqrt{h}}{a_l\sqrt{n}}\sigma_0. \tag{22}$$

According to the statistical results from Table 3, $\sigma_F = 0.0156\sigma_0$, which signifies that the noise level has been reduced about 18 dB.

The Lyapunov exponent distribution for a large-scale periodic state is shown in Figure 5.

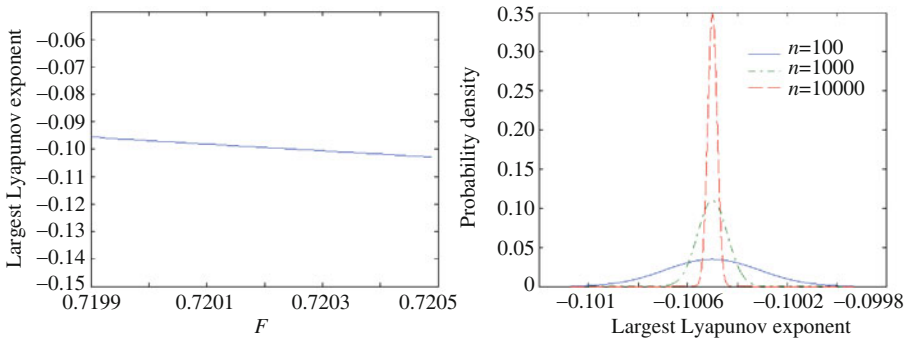

Figure 5 Lyapunov exponent distribution for a large-scale periodic state.

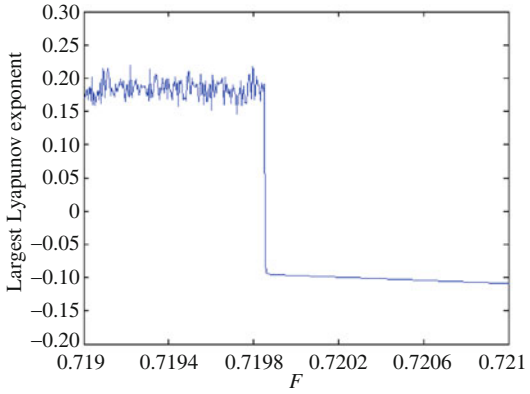

Figure 6 Lyapunov exponent for a critical state.

3.3.4 *Statistical characteristics of the Lyapunov exponent for a critical state*

At the critical point, the Lyapunov exponent will reverse sign from positive to negative. Thus, the Lyapunov exponent and F_r can be linearly fitted by a nearly vertical line. When the driving force changes from 0.71985475775012 to 0.71985475775014, the Lyapunov exponent decreased from positive to negative, as detailed in Figure 6.

When we put (13) and (14) into (17), the Lyapunov exponent for a critical state with perturbing input noise can be represented by (23).

$$\lambda_2 = \lambda_p + n_p = \lambda_p + \frac{R_p\sqrt{h}}{\sqrt{n}} n_\sigma, \tag{23}$$

where λ_p is the average value of the Lyapunov exponent for a critical state, n_p its frustration, and R_p its critical ratio to input noise. Similarly, λ_p is a variable depending on the driving force threshold F_r accompanied by a large rate of change. Statistical results show that when k=0.5, $F_r = 0.719854757750125$, h=0.01 and n=100, the values of the parameters in (23) are: $\lambda_p = -0.007019$ and $R_p = 1.019 \times 10^{13}$. By linear fitting, the Lyapunov exponent can be represented by:

$$\lambda_p = -a_p F + b_p, \tag{24}$$

where a_p and b_p are fitting parameters. According to the statistical results from Table 4, their values are found to be $a_p = 5.256 \times 10^{12}$ and $b_p = 3.786 \times 10^{12}$. In a manner similar to the above, we find the relationship between input noise and frustration to be

$$\sigma_F = \frac{R_p\sqrt{h}}{a_p\sqrt{n}} \sigma_0. \tag{25}$$

Table 4 Statistical results of the Lyapunov exponent for a critical state

F_r	h	n	σ_0	Mean value	Standard deviation
0.719854757750125	0.01	100	10^{-28}	0.007019	1.019e−3
		1000		0.006817	3.364e−4
		10000		0.006927	1.613e−4
0.719854757750125	0.01	100	10^{-29}	0.006964	3.352e−4
			10^{-30}	0.006979	1.568e−4

Based on this equation and parameter values, $\sigma_F = 0.0194\sigma_0$. The value is similar to that for the large-scale periodic state, signifying that the perturbing input noise is fixed in these states.

3.4 Statistical characteristics of the Lyapunov exponent

Based on (17), the statistical characteristics of the Lyapunov exponent can be summarized by the following equations:

$$\begin{cases} \lambda_1 = \lambda_c + \dfrac{R_c}{\sqrt{n}} n_0, & F < F_1, \\ \lambda_2 = -a_p F + b_p + \dfrac{R_p\sqrt{h}}{\sqrt{n}}\sigma_0, & F_1 \leqslant F < F_2, \\ \lambda_3 = -a_l F + b_l + \dfrac{R_l\sqrt{h}}{\sqrt{n}}\sigma_0, & F \geqslant F_2, \end{cases} \tag{26}$$

where $a_p = 5.256 \times 10^{12}$, $b_p = 3.786 \times 10^{12}$, $a_l = 12.2809$, $b_l = 8.7454$, $R_c = 0.137$, $R_l = 19.1$ and $R_p = 1.019 \times 10^{13}$.

4 Signal detection and estimation based on chaotic oscillator

4.1 Weak signal detection based on the chaotic oscillator

4.1.1 *Neyman-Pearson principle*

The Neyman-Pearson principle [26] is commonly used in signal detection theory. Our study also uses this principle to analyze the chaotic signal detection system associated with the Duffing oscillator. For a common signal detection problem, there are two hypotheses:

$$\begin{cases} H_{s0}: & x(t) = n_\sigma(t), \\ H_{s1}: & x(t) = A\cos(\omega t) + n_\sigma(t), \end{cases} \tag{27}$$

where $n_\sigma(t) \sim N(0, \sigma_0)$. The first hypothesis indicates an absence of a weak signal while the second includes such a signal. According to (16), if n time tests have been performed for H_s, the k-th test result is equivalent to the following hypotheses:

$$\begin{cases} H_{F0}: & F[k] = F_r + n_F[k], \\ H_{F1}: & F[k] = F_r + A + n_F[k], \end{cases} \tag{28}$$

where $n_F(t) \sim N(0, \sigma_F)$. Because $F[k]$ cannot be measured directly, the criterion can be performed by the mapping between F and the Lyapunov exponent. The two hypotheses based on the Lyapunov exponent are:

$$\begin{cases} H_{l0}: & \lambda[k] \geqslant 0, \\ H_{l1}: & \lambda[k] < 0. \end{cases} \tag{29}$$

(29) is equivalent to following hypotheses:

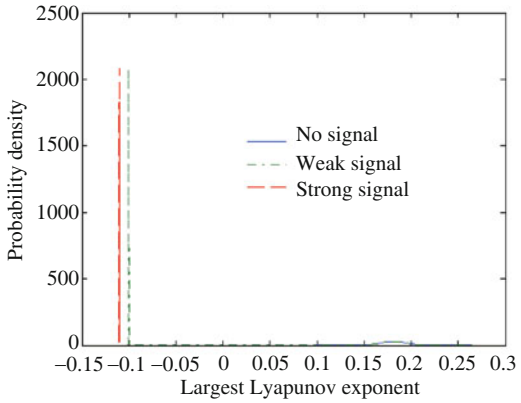

Figure 7 Lyapunov exponent distributions in weak signal detection.

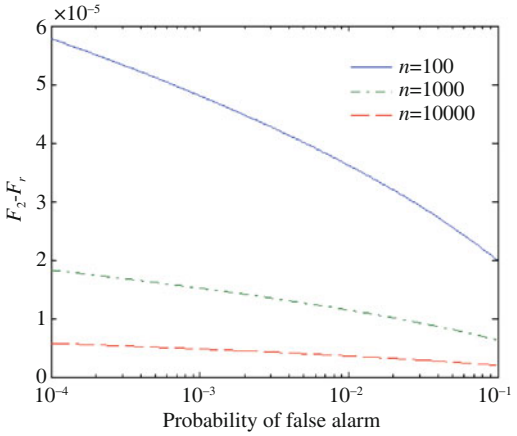

Figure 8 Relationship between false alarm probability and driving force.

$$\begin{cases} H_{l0}: & F[k] \leqslant F_2, \\ H_{l1}: & F[k] > F_2. \end{cases} \tag{30}$$

The probability distributions of the Lyapunov exponent under different kinds of inputted signals are shown in Figure 7.

4.1.2 *False alarm probability*

$P(H_{l1}; H_{s0})$ is used to denote the probability that the value of the Lyapunov exponent is larger than zero in the absence of an input signal. Because n_f follows a normal distribution, the false alarm probability is then represented by

$$\begin{aligned} P_{fa} = P(H_{l1}; H_{s0}) &= P(F[k] > F_2; H_{s0}) \\ &= \int_{F_2}^{+\infty} \frac{1}{\sqrt{2\pi\sigma_F^2}} \exp\left[-\frac{1}{2\sigma_F^2}(k - F_r)^2\right] \mathrm{d}k \\ &= \frac{1}{2}\mathrm{erfc}\left(\frac{F_2 - F_r}{\sqrt{2}\sigma_F}\right) \\ &= \frac{1}{2}\mathrm{erfc}\left(\frac{a_l\sqrt{n}}{R_l\sqrt{h}}\frac{F_2 - F_r}{\sqrt{2}\sigma_0}\right). \end{aligned} \tag{31}$$

For a specified Duffing equation, parameters R_l, a_l and F_2 are stable. The false alarm probability can be reduced by three methods: increasing the sampling time n, decreasing the sampling interval h, and decreasing the driving force threshold F_r. The relationship between F_r and P_{fa} can be represented by

$$F_r = F_2 - \sqrt{2}\sigma_0 \frac{R_l\sqrt{h}}{a_l\sqrt{n}}\mathrm{erfc}^{-1}(2P_{fa}). \tag{32}$$

When h=0.01 and input noise $\sigma_0^2 = 10^{-6}$, the relationship between the false alarm probability and the driving force for different sampling times n is displayed in Figure 8.

If the probability of false alarms is 1%, then $F_2 - F_r = 3.618 \times 10^{-5}$ yielding F_r should be 0.7198186.

4.1.3 *Detection probability*

$P(H_{l1}; H_{s1})$ is used to represent the probability that the Lyapunov exponent is negative in the absence of an input signal. Again, as n_f follows a normal distribution, the detect probability of the system is

$$\begin{aligned} P_d &= P(H_{l1}; H_{s1}) = P(F[k] > F_2; H_{s1}) \\ &= \int_{F_2}^{+\infty} \frac{1}{\sqrt{2\pi\sigma_F^2}} \exp\left[-\frac{1}{2\sigma_F^2}(k - F_r - A)^2\right] \mathrm{d}k \\ &= \frac{1}{2}\mathrm{erfc}\left(\frac{F_2 - F_r - A}{\sqrt{2}\sigma_F}\right) \\ &= \frac{1}{2}\mathrm{erfc}\left(\frac{a_l\sqrt{n}}{R_l\sqrt{h}}\frac{F_2 - F_r - A}{\sqrt{2}\sigma_0}\right). \end{aligned} \tag{33}$$

Similarly, the detect probability can be increased by increasing sampling time n, decreasing sample interval h, or increase driving force threshold F_r. The relationship between F_r and P_d can be represented by

$$A = F_2 - F_r - \sqrt{2}\sigma_0\frac{R_l\sqrt{h}}{a_l\sqrt{n}}\mathrm{erfc}^{-1}(2P_d). \tag{34}$$

When h=0.01 and input noise $\sigma_0^2 = 10^{-6}$, the relationship between the detection probability and input signal A for different sampling times n is shown in Figure 9.

If the detection probability is set at 99%, the signal amplitude is $A = 7.2362 \times 10^{-5}$, which yields detection of SNR= $20\log_{10}(\frac{A}{\sigma_0}) = -22.8$ dB.

4.1.4 *Detection signal to noise ratio* (SNR)

Putting (34) into (32), we obtain the signal to noise ratio given false alarm probability P_{fa} and detection probability P_d:

$$\begin{aligned} A &= F_2 - F_r - \sqrt{2}\sigma_0\frac{R_l\sqrt{h}}{a_l\sqrt{n}}\mathrm{erfc}^{-1}(2P_d) \\ &= \sqrt{2}\sigma_0\frac{R_l\sqrt{h}}{a_l\sqrt{n}}(\mathrm{erfc}^{-1}(2P_{fa}) - \mathrm{erfc}^{-1}(2P_d)), \\ \frac{A}{\sigma_0} &= \sqrt{2}\frac{R_l\sqrt{h}}{a_l\sqrt{n}}(\mathrm{erfc}^{-1}(2P_{fa}) - \mathrm{erfc}^{-1}(2P_d)). \end{aligned} \tag{35}$$

(35) shows the detection SNR will continuously increase with increasing sampling rate and sampling time.

4.2 Signal estimation based on chaotic oscillator

Similarly for signal detection, the signal amplitude can be estimated based on the Lyapunov exponent. If the input signal is too low, the Duffing oscillator will remain in a chaotic state. The Lyapunov exponent does not reflect the input signal strength. Thus, the signal estimation works mainly for large-scale periodic states. According to (21), the amplitude of the input signal can be measured by the following expressions:

$$\lambda_3 = -a_l(F_r + A) + b_l + \frac{R_l\sqrt{h}}{\sqrt{n}}n_\sigma, \tag{36}$$

$$A = -\frac{\lambda_3 - b_l}{a_l} - F_r + \frac{R_l\sqrt{h}}{a_l\sqrt{n}}n_\sigma. \tag{37}$$

The accuracy of the estimation can be expressed as follows:

$$E(\hat{A}) = -\frac{\lambda_3 - b_l}{a_l} - F_r, \tag{38}$$

$$\mathrm{var}(\hat{A}) = \frac{R_l^2 h}{a_l^2 n}n_\sigma^2. \tag{39}$$

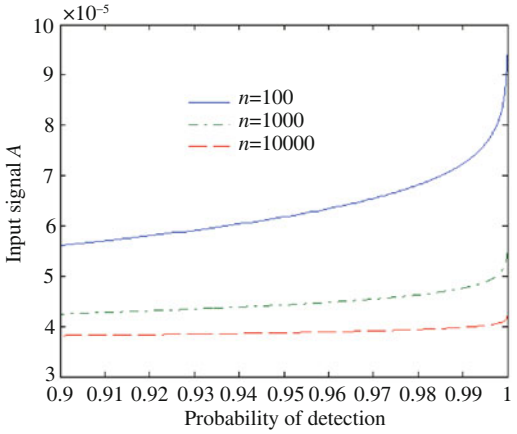

Figure 9 Relationship between input signal amplitude and detection probability.

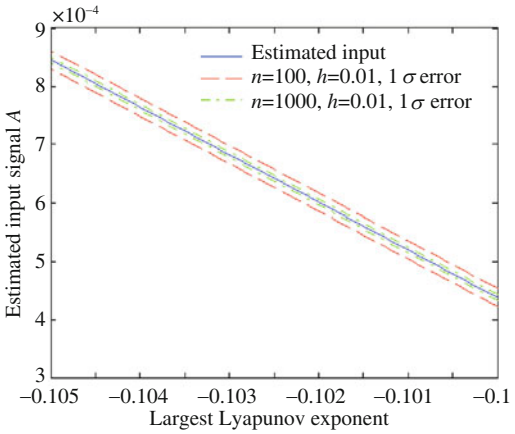

Figure 10 Signal amplitude estimation based on the Lyapunov exponent.

To increase the accuracy of the signal amplitude estimation, either increasing the sampling time or decreasing the sampling interval is still feasible. Specifying the input noise $\sigma_0^2 = 10^{-6}$, the estimation dependence is shown in Figure 10.

5 Conclusions

Previous studies have used the Lyapunov exponent as a criterion in chaotic weak signal detection systems. However, noise affecting chaotic state evaluations was not considered in those papers and this has lead to inaccuracies in signal detection and high false alarm probabilities. To mitigate these problems, we studied the statistical characteristics of weak signal detection based on the chaotic Duffing oscillator, clarified the factors affecting the Lyapunov exponent calculation, and built up a model that treats the connection between Lyapunov exponents and input noise. The parameters in the model were calculated by simulation of a modified Duffing-Holmes equation. Furthermore, the calculation methods to obtain false alarm probabilities, detection probabilities and detection SNRs are demonstrated using this model, and extended into weak signal amplitude estimation. This paper contributes in extending the statistical signal detection and estimation theory into the area of chaotic signal detection. It also points out the inconsistency in directly using Lyapunov exponents as a criterion for chaotic weak signal detection in noisy backgrounds, and shows how to exploit probability and statistical methods to describe the performance of chaotic weak signal detection systems.

Acknowledgements

This work was supported by the National High-Tech Research & Development Program of China (Grant No. 2009AA12Z313) and State Laboratory of Software Development Environment Open Fund.

References

1 Birx D L, Pipenberg S J. Chaotic oscillators and complex mapping feed forward networks (CMFFNs) for signal detection in noisy environments. In: International Joint Conference on Neural Networks, New York: IEEE Neutral Networks Council, 1992. 881–888
2 Haykin S, Xiao B L. Detection of signals in chaos. Proc IEEE, 1995, 83: 95–122
3 Leung H, Huang X. Parameter estimation in chaotic noise. IEEE Trans Signal Process, 1996, 44: 2456–2463
4 Kennedy M P, Kolumban G. Digital communications using chaos. Signal Process, 2000, 80: 1307–1320
5 Short K M. Signal extraction from chaotic communication. Int J Bifurcation Chaos. 1997, 7: 1579–1597

6 Wang G, Lin J, Chen X, et al. The application of chaotic oscillators to weak signal detection. IEEE Trans Ind Electron, 1999, 46: 440–444

7 Wang G, Zheng W, He S. Estimation of amplitude and phase of a weak signal by using the property of sensitive dependence on initial conditions of a nonlinear oscillator. Signal Process, 2002, 82: 103–115

8 Wang F P, Guo J B, Wang Z J, et al. Harmonic signal extraction from strong chaotic interference (in Chinese). Acta Phys Sinica, 2001, 50: 1019–1023

9 Li Y, Xu K, Yang B J, et al. Analysis of the geometric characteristic quantity of the periodic solutions of the chaotic oscillator system and the quantitative detection of weak periodic signal (in Chinese). Acta Phys Sinica, 2008, 57: 3353–3358

10 Li Y, Yang B J, Lin H B, et al. Simulation and theoretical analysis on detection of the frequency of weak harmonic signals based on a special chaotic system (in Chinese). Acta Phys Sinica, 2005, 54: 1994–1999

11 Li Y, Yang B J, Shi Y W. Chaos-based weak sinusoidal signal detection approach under colored noise background (in Chinese). Acta Phys Sinica, 2003, 52: 526–530

12 Liu Q Z, Song W Q. Detection weak period signal using chaotic oscillator. In: Computational Science and Its Applications (ICCSA 2009), Berlin: Springer, 2009. 685–692

13 Dubuc B, Quiniou J F, Roques-Carmes C, et al. Evaluating the fractal dimension of profiles. Phys Rev A: At Mol Opt Phys, 1989, 39: 1500–1512

14 Kolmogorov A N. New metric invariant of transitive dynamical systems and endomorphisms of lebesgue spaces. Dokl Russ Acad Sci, 1958, 119: 861–864

15 Pecora L M, Carroll T L, Johnson G A, et al. Fundamentals of synchronization in chaotic systems, concepts, and applications. Chaos Interdisciplinary J Nonlinear Sci, 1997, 7: 520–543

16 Zhang B, Li Y, Ma H T. An algorithm based on Lyapunov exponents to determine the threshold of chaotic detection for weak signal (in Chinese). Progress Geophys, 2003, 04: 748–751

17 Lu S, Wang H Y. Calculation of the maximal Lyapunov exponent from multivariate data (in Chinese). Acta Phys Sinica, 2006, 55: 572–576

18 Xu W, Guo J B. Detection of chaotic direct sequence spread spectrum signal based on the largest lyapunov exponent (in Chinese). J Appl Sci, 2009, 27: 111–116

19 Zhang B, Li Y, Lu J. Study of the Lyapunov characteristic exponents used as the criteria for chaos (in Chinese). J Jilin University (Inf Sci Ed). 2004, 22: 111–114

20 Moon F C, Holmes P J. A magnetoelastic strange attractor. J Sound Vib, 1979, 65: 275–296

21 Wang G Y, Chen D J, Lin J Y, et al. The statistical characteristics of weak signal detection based on Duffing oscillator (in Chinese). Acta Electronica Sinica, 1998, 10: 38–44

22 Grassberger P, Procaccia I. Characterization of strange attractor. Phys Rev Lett, 1983, 50: 346–349

23 Wolf A, Swift J B, Swinney H L, et al. Determining Lyapunov exponents from a time series. Physica D, 1985, 16: 285–317

24 Rosenstein M T, Collins J J, de Luca C J. A practical method for calculating largest Lyapunov exponents from small data sets. Physica D, 1993, 65: 117–134

25 Liu W J. Probability and Mathematics Statistic. Beijing: Tsinghua University Press, 2005. 82

26 Neyman J, Pearson E S. On the problem of the most efficient tests of statistical hypotheses. Philos Trans R Soc London, Ser A, 1933, 231: 289–337